JOURNAL OF CATALYSIS 42, 181–196 (1976)

The Dehydrogenation and Hydrogenolysis of Cyclohexane and Cyclohexene on Stepped (High Miller Index) Platinum Surfaces

D. W. BLAKELY[1] AND G. A. SOMORJAI

Inorganic Materials Research Division, Lawrence Berkeley Laboratory, and Department of Chemistry, University of California, Berkeley, California 94720

Received August 19, 1975

The dehydrogenation and hydrogenolysis of cyclohexane and cyclohexene were studied on platinum single crystal surfaces of varying atomic surface structure at low pressures (10^{-6} Torr) in the temperature range of 300–723 K. The quantitative reaction rates were monitored by a mass spectrometer, the surface structure and surface composition were determined by low-energy electron diffraction and Auger electron spectroscopy. Atomic steps have been identified as the active sites for C–H and H–H bond breaking processes. The dependence of the dehydrogenation and hydrogenolysis rates on the platinum surface structure revealed kinks in the steps as active sites for C–C bond scission in addition to their ability for breaking C–H and H–H bonds. The active catalyst surface was covered with a carbonaceous overlayer, which was ordered or disordered. The properties of this overlayer influence significantly both the rate and the product distribution of the catalytic reactions. An expanded classification of structure-sensitive reactions is suggested.

INTRODUCTION

One of the important aims of studies of hydrocarbon catalysis is to uncover the sites where C–H, C–C, and H–H bonds are broken followed by suitable rearrangements of the hydrocarbon fragments. Identification of these active centers might permit the architecture of catalyst surfaces with optimum concentrations of surface sites with a variety of bond breaking activities.

The dehydrogenation and hydrogenolysis of cyclohexane and cyclohexene were studied on platinum single crystal surfaces at low pressures [about 10^{-6} Torr (1 Torr = 133.3 N/m^2)] to find the correlation between the reactivity and the atomic surface structure. We report the discovery and identification of two such surface sites on platinum crystal surfaces that differ in the number of nearest neighbor platinum atoms surrounding them. H–H and C–H bond breaking processes predominate at one of the sites while C–C bond breaking occurs in addition to breaking H–H and C–H bonds at the other. We also present evidence that during the catalytic reactions the platinum surface is partially or completely covered with a layer of carbonaceous deposit, ordered or disordered, whose properties play a significant role in determining both the resistance to poisoning and product distribution during the catalytic reactions.

The reactions of cyclohexane and cyclohexene are well suited for identifying active surface sites with various bond breaking activities for several reasons. The de-

---

[1] Department of Chemical Engineering, University of California, Berkeley. Present address: Chevron Research Co., P. O. Box 1627, Richmond, California 94802.

hydrogenation occurs rapidly at relatively low temperatures and at low partial pressures of hydrogen, since it is thermodynamically favored at these conditions. Since dehydrogenation requires only C–H bond breaking activity, the effectiveness of the platinum crystal surfaces to breaking C–H bonds could be investigated in a systematic manner. The appearance of hydrogenolysis products such as *n*-hexane would signal the presence of sites with C–C bond breaking activity. Since the mass spectra of benzene and *n*-hexane are readily distinguishable from cyclohexane both the dehydrogenation and hydrogenolysis activity of a given crystal face were readily monitored using a quadrupole mass spectrometer.

The dehydrogenation of cyclohexane, cyclohexene, and cyclohexadiene on the Pt(111) crystal face has recently been studied in this laboratory (*1*). The (111) crystal face of platinum is catalytically quite inactive; it apparently lacks the active sites that must be present in large enough concentration for efficient dehydrogenation and hydrogenolysis. Both cyclohexane and cyclohexene were maintained on the surface without much dehydrogenation at 300 K and their ordered surface structures were identified. Cyclohexadiene, however, instaneously dehydrogenated to benzene even on this inactive platinum surface. The rate-limiting steps in dehydrogenating cyclohexane to benzene was the dehydrogenation of the cyclohexene intermediate. The Pt(111) crystal face will not dehydrogenate cyclohexane beyond cyclohexene even at higher temperatures (>425 K).

In this paper it is shown that the reactivity of cyclohexane and cyclohexene is entirely different on platinum surfaces with a high concentration of atomic steps than it is on the (111) crystal face; in this case these molecules dehydrogenate readily. Atomic steps, which were found responsible for breaking H–H bonds in studies of hydrogen–deuterium exchange (*2*), were also effective in breaking the C–H bonds. It appears that atomic steps are the active sites on platinum surfaces for performing these important bond scissions. The atomic surface structures where C–C bond scissions occur efficiently, in addition to C–H and H–H bond scissions, have been identified as kinks in steps. The quantitative reaction rates (as turnover numbers) for dehydrogenation and hydrogenolysis were determined and correlated with the various atomic surface structures. Thus, the structure insensitivity of the cyclohexane to cyclohexene dehydrogenation reaction, and the structure-sensitivity of the dehydrogenation of cyclohexene and hydrogenolysis of cyclohexane have been established.

EXPERIMENTAL METHODS

The measurements of the dehydrogenation and hydrogenolysis rates of cyclohexane and cyclohexene were carried out at low pressures (10^{-7}–10^{-6} Torr total pressure) in the presence of excess hydrogen. The hydrogen to hydrocarbon ratio was varied to investigate the hydrogen pressure dependence of the reaction rate. The temperature range of our studies was 300–725 K. The schematic of the low pressure reaction chamber is shown in Fig. 1. It is equipped with UTI 100C quadrupole mass spectrometer that is placed about 5 cm from the single crystal

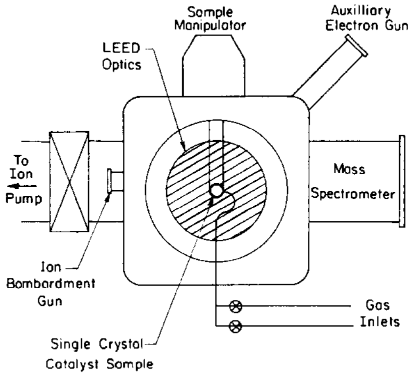

FIG. 1. Schematic diagram of reaction chamber used for low pressure catalytic reaction studies.

TABLE 1

Angle of Cut, Miller Indices and Designation of Stepped Platinum Surfaces

Angle of cut (°)	Miller index	Designation
0 from $(\bar{1}11)$	$(\bar{1}11)$	Pt-(111)
9.5 from $(\bar{1}11)$	$(\bar{5}57)$	Pt(S)-[6(111) × (100)]
19.5 from $(\bar{1}11)$	$(\bar{1}12)$	Pt(S)-[3(111) × (100)]
9.5 from $(\bar{1}11)$ rotated 7°	$(\overline{11}, 12, 16)$	Pt(S)-[6(111) × (710)]
9.5 from $(\bar{1}11)$ rotated 20°	$(\bar{6}79)$	Pt(S)-[7(111) × (310)]
6.2 from (001)	$(\bar{1}, 1, 13)$	Nominally, Pt(S)-[7(100) × (111)] facets to (100) and (311) planes

catalyst surface. The two catalyst samples mounted in the center of the chamber may be independently heated resistively to 1900 K, if desired. The presence of the second carbon-contaminated catalyst sample at ambient temperature does not affect the reaction rate measured for the sample under study. Each single crystal catalyst sample has approximately 0.8 cm^2 of surface area. Hydrogen and the hydrocarbon reactant may be introduced into the reaction chamber independently by the use of two variable leak values. The gases in the 15 liter reaction chamber are well-mixed since the mean free path (approx. 20 m at 8×10^{-7} Torr) of the reactant is much larger than the dimensions of the chamber. The reaction chamber is equipped with low-energy electron diffraction optics for studying the structures of the catalyst surface and adsorbates, with a retarding potential Auger electron spectrometer to monitor the surface composition, and an ion bombardment gun for ion sputter removal of unwanted surface impurities.

The ultrahigh vacuum pumping system consisted of a 140 liter/sec Vac-Ion pump and a titanium getter pump which could be independently isolated by gate valves. Ultrahigh vacuum of 5×10^{-10} Torr could readily be achieved after baking the chamber walls to 250°C.

The platinum single crystal catalyst samples used in this study were prepared from three different single crystal rods obtained from different manufacturers, Materials Research Corp. and Research Organic/Inorganic Chemical Corp. The rods contained different impurities (carbon and calcium; carbon and phosphorus; and carbon, phosphorus and sulfur) which when removed gave a reproducible catalyst surface both by low-energy electron diffraction and the catalytic reaction rates.

The catalyst samples were prepared by orienting with a Laue back-reflection X-ray technique, spark cutting an approximately 1 mm thick slice with the proper crystallographic orientation exposed, polishing both sides and etching. The carbon, phosphorous and sulfur impurities could be removed by oxidation in 5×10^{-8} Torr of oxygen at 1075 K. The adsorbed oxygen was removed by heating the samples to 1375 K in vacuum. A high concentration of calcium impurity, which possibly remained in the sample from the reduction of the platinum ore, could only be removed by extensive oxidative heat treatments. The sample was oxidized at 1500 K in 10^{-5} Torr of oxygen for 24–48 hr. This treatment fixes the calcium on the surface in the form of a stable oxide which will decompose with calcium vaporization from the surface with brief heating to 1900 K. A small calcium impurity may be removed also by argon ion bombardment and 1100 K anneal cycles. The clean platinum surface structure

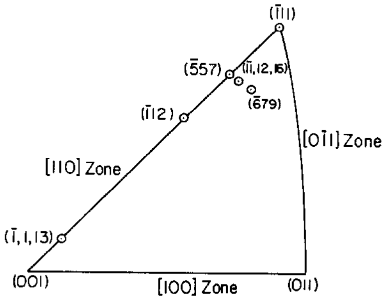

FIG. 2. Crystallographic orientation and Miller index of the platinum single crystal catalyst surfaces studied.

can be identified by both the low-energy electron diffraction pattern and the Laue X-ray diffraction pattern. Table 1 lists the orientations of various crystal faces that are used in these studies with the notation that is described, in detail, elsewhere (*3*). In brief, (S) indicates a stepped surface; [6(111) × (100)], for example, identifies a surface with atomic terraces of (111) orientation six atoms wide, on the average, separated by steps of monatomic height of (100) orientation (deduced from the direction of the cut). The orientation of the samples on the unit stereographic triangle is shown in Fig. 2.

The first five samples differ only in the step density and the number of kinks in the steps, all catalysts having (111) orientation terraces and monatomic height steps. The fourth and fifth catalyst samples were obtained by cutting the crystal rod off the [110] zone toward the $[0\bar{1}1]$ zone. The sixth sample was cut to expose (100) orientation terraces. The (100) orientation surface of platinum reconstructs to form a buckled hexagonal layer of platinum atoms atop of the square bulk lattice charac-

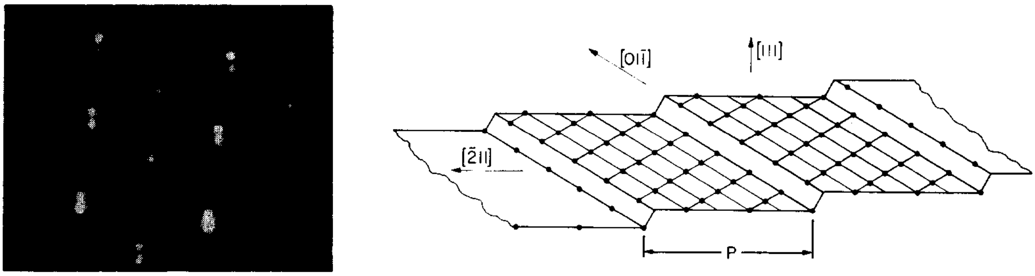

A. Pt(S)-[6(111)x(100)]

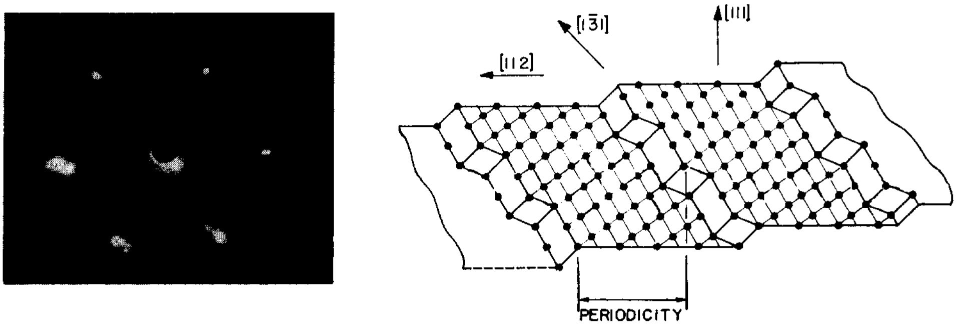

B. Pt(S)-[7(111)x(310)]

FIG. 3. Low-energy electron diffraction patterns and schematic representation of: (a) Pt(S)-[6(111) × (100)] which has a step density of 2.5 × 10^{14} step atoms/cm^2 and (b) Pt(S)-[7(111) × (310)], step density of 2.3 × 10^{14} atoms/cm and kink density of 7 × 10^{13} atoms/cm^2.

terized by a (5 × 20) low-energy electron diffraction pattern (*4*). This surface was stable in monatomic height step configuration. The relative structural stabilities of the various high Miller index surfaces will be discussed further in a subsequent paper (*5*).

Figure 3 shows schematic diagrams and the observed diffraction patterns of two catalytically representative stepped catalyst surfaces. In Fig. 3a a catalyst surface with straight steps of monatomic height and a 6 atom wide terrace giving a step atom density of 2.5×10^{14} atoms/cm^2, 18% of the total number of surface atoms, Pt(S)-[6(111) × (100)], is shown. While the catalyst in Fig. 3b has the same terrace width and step density, there are kinks in the steps with a density of 7×10^{13} atoms/cm^2 (or 30% of the total number of step atoms, 5% of the total surface). The step height is obtained from the variation of the intensity maxima of the doublet diffraction beam features with electron energy which has been discussed elsewhere (*6*). After catalytic reactions of hydrocarbons, the catalyst surface could be readily regenerated. The carbon deposits were removed by oxygen heat treatment and subsequent removal of oxygen by vacuum reduction. The purity of the catalyst surface was checked by Auger electron spectroscopy before each run.

After the catalyst sample is cleaned, the temperature is lowered to reaction temperature and hydrogen is introduced to the reaction chamber at the desired flow rate, 3×10^{14} molecules/sec. The valve to the ion pump is then partially closed to reduce the pumping speed to approximately 2 liters/sec and increase the hydrogen pressure to 8×10^{-7} Torr. Background mass spectra are taken and the hydrocarbon, cyclohexane or cyclohexene, is introduced through a separate valve to a pressure of 4×10^{-8} Torr. The standard conditions for the measurements taken in this study are 4×10^{-8} Torr of hydrocarbon reactant, 8×10^{-7} Torr of hydrogen and 2 liters/sec pumping speed. Under these flow conditions, a reactant hydrocarbon molecule strikes the catalyst surface, on the average, approximately five times before it is pumped and conversions are 1–2% for cyclohexane and 1–50% for cyclohexene. With the valve to the ion pump partially closed to give a conductance of approximately 2 liters/sec, there is very little backstreaming of decomposition products from the ion pump (*7*). The rates for backstreaming and reaction with the chamber walls have been monitored in blank control reactions and are less than 10% of the rate of production of any reaction product except methane where it is approximately 80%. The mass spectrometer was used to monitor the partial pressures of reactant and product gases and was calibrated using the nude ionization gauge as a standard for all the hydrocarbons. The temperature of the catalyst was measured with a platinum/platinum–10% rhodium thermocouple spot welded to the top edge of the crystal. After the run was finished the conductance of the valve to the ion pump for hydrogen was measured so the reaction rate could be quantified. The reactions rates were calculated using the measured pumping speed and partial pressures in the equation for a back mixed reactor (*8*),

$$R_i = 3.2 \times 10^{16} S P_i, \tag{1}$$

where R_i is rate of production of product i (molecules/sec), S is the pumping speed (cm^3/sec) and P_i is the partial pressure of i-th product (Torr). Auger electron spectra were taken only after the reaction mixture was pumped from the chamber. Low-energy electron diffraction observations could be made during a reaction without affecting the reaction rate or observed diffraction pattern. Dehydrogenation reactions were studied, since at the low hydrogen pressures used, equilibrium greatly favors the de-

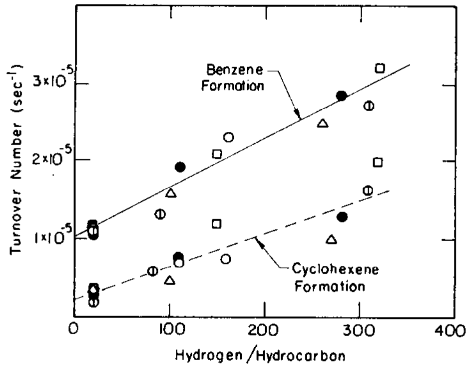

FIG. 4. Initial steady state rate of production of benzene (——) and cyclohexene (- - -) from cyclohexane. The reaction conditions are 4×10^{-8} Torr of cyclohexane and 423 K catalyst temperature (△) Pt(S)-[7(100) × (111)];(□) Pt(S)-[3(111) × (100)]; (○) Pt(S)-[6(111) × (100)]; (⦶) Pt(S)-[6(111) × (710)]; (●) Pt(S)-[7(111) × (310)].

hydrogenated products cyclohexene and benzene over cyclohexane.

RESULTS

A. The Dehydrogenation and Hydrogenolysis of Cyclohexane

In a series of studies, we have determined the variation of the turnover number, the number of product molecules per platinum surface atoms per second, with the hydrogen to hydrocarbon ratio at a constant hydrocarbon pressure of 4×10^{-8} Torr. The results are shown in Fig. 4 for the several stepped surfaces studied. The variation is very similar for all catalyst surfaces. The reaction rates increase with increasing hydrogen to hydrocarbon ratio. If no hydrogen is introduced into the reaction chamber the catalyst behaves very differently. No benzene is produced and cyclohexene production is reduced greatly. There is also a higher than normal amount of carbon residue on the surface, approximately one monolayer. Pretreating the catalyst in hydrogen and then removing it prior to hydrocarbon introduction does not increase the activity for dehydrogenation or hydrogenolysis.

We shall present the results of the reaction rate studies for dehydrogenation and hydrogenolysis that were obtained on stepped platinum surfaces first. Then we shall present the same rate data obtained for stepped surfaces which have a large concentration of kinks in the step. In Fig. 5a the turnover number for dehydrogenation to benzene at 20 to 1 hydrogen to hydrocarbon ratio and hydrogenolysis to *n*-hexane at 300 to 1 hydrogen to hydrocarbon ratio are shown as a function of step density at 423 K. The dehydrogenation rate is independent of step density, while the hydrogenolysis rate increases with increased step density. The hydrogenolysis rate that was measured via the rate of formation of *n*-hexane, one of the hydrogenolysis products, was lower than the rate of dehydrogenation to benzene. The molar hydrogenolysis product distribution (satur-

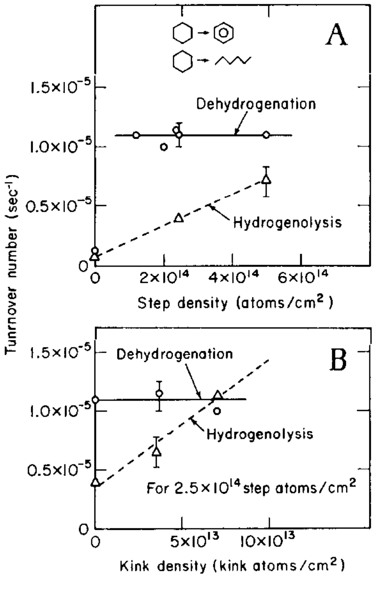

FIG. 5. Cyclohexane dehydrogenation to benzene (○) and hydrogenolysis to *n*-hexane (△) as a function of (A) step density and (B) kink density. The rates of hydrogenolysis per surface site are the slopes of the lines representing hydrogenolysis and are 2.5×10^{-4} molecules of *n*-hexane/kink atom/sec and 2×10^{-5} molecules/step atom/sec. (The slope is multiplied by 1.5×10^{-15} Pt atoms/cm² to obtain the desired units.)

ated aliphatic hydrocarbons only), appears to be $C_6:C_3:C_1 = 1:1:4$. Even though *n*-hexane is a minority hydrogenolysis product, it is a reliable measure of the degree of hydrogenolysis because of its ease of mass spectrometric detection and it is not formed in a background reaction with the walls of the reaction chamber. Besides the saturated hydrogenolysis products and benzene, we find the olefinic products cyclohexene, ethylene, and propylene. Cyclohexene is an intermediate in the dehydrogenation to benzene and its various reactions are discussed separately in the next section. The olefinic product distribution of ethylene:propylene:cyclohexene:benzene is 10:1:0.5:1.

The turnover numbers for dehydrogenation and hydrogenolysis on kinked surfaces are shown in Fig. 5b. The kink density is defined as the number of kink sites per square centimeter (the total number of atoms on the surface is approximately $1.5 \times 10^{15}/cm^2$). For example, on the Pt(S)-[7(111) × (310)] surface every third atom along the step should, on the average, be in a kink position. Therefore, for this surface the step density is $2.0 \times 10^{14}/cm^2$ and the kink density is approximately $7 \times 10^{13}/cm^2$. By comparing the turnover numbers with those obtained from stepped surfaces that were shown in Fig. 5a, it appears that the rate of hydrogenolysis is markedly higher in the presence of kinks. The rate of cyclohexane hydrogenolysis to *n*-hexane at a kink atom is 2.5×10^{-4} molecules/kink atom/sec. This is almost an order of magnitude higher than the rate at a step atom, 2×10^{-5}/sec. The dehydrogenation rate is approximately constant and remains unaffected by variation of kink density while the hydrogenolysis rate increases by an order of magnitude from a surface free of steps, Pt(111). The kinks in the stepped surface appear to be very effective in breaking C–C bonds leading to much enhanced hydrogenolysis rates. The hydrogenolysis product distributions do not change appreciably with step or kink density, only the rate increases. The independence of the dehydrogenation rate from the step and kink density shows that this reaction is indeed structure-insensitive. The hydrogenolysis rate increases with kink density just as with increasing step density, thus, hydrogenolysis appears to be structure-sensitive.

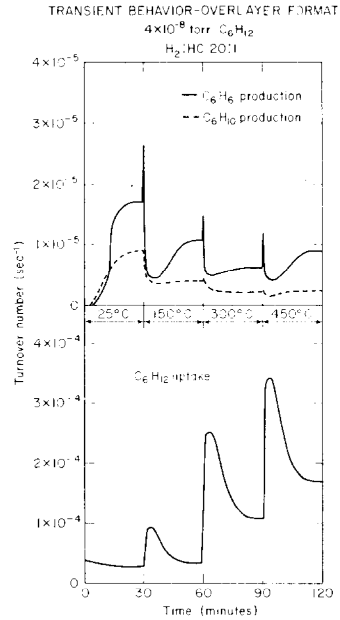

FIG. 6. Induction period for production of benzene (——) and cyclohexene (– – –) from cyclohexane. Hydrogen:cyclohexane ratio, 20:1; cyclohexane pressure, 4×10^{-8} Torr.

There was always an induction period of 10–20 min before the benzene product reached its steady state rate of production as detected by the mass spectrometer after the introduction of cyclohexane onto the crystal surface. This is shown in Fig. 6 for several catalyst temperatures. The catalyst was initially at 300 K. When steady state reaction rates were obtained, the catalyst temperature was rapidly increased (in approx 30 sec) to 423 K and the reaction rate was monitored. This was repeated with heating to 573 and 723 K. The benzene desorbed during rapid heating of the

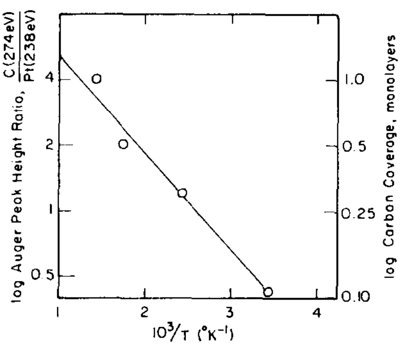

FIG. 7. The amount of carbon on the catalyst surface at steady state reaction under standard conditions. An Auger peak height ratio of 4.0 corresponds to approximately 1.0 monolayer of carbon. Line through points has a 2 kcal/mole slope.

catalyst surface is approximately 1 × 10^{13} molecules or less and represents only a small fraction of the carbon on the surface. The steady state reaction rates at a given temperature are the same whether the catalyst was initially at that temperature or another. This induction period coincides with a higher than steady state uptake of cyclohexane. A mass balance calculation on carbon, utilizing the known adsorption and desorption rates of reactants and products during the induction period indicated carbon was deposited on the surface. The amount calculated agreed reasonably well with that determined by the Auger electron spectra taken after the reaction mixture was pumped from the chamber, since the electron beam may induce polymerization of hydrocarbons and further carbon deposition. The formation of the adsorbed carbon layer always precedes the desorption of benzene and olefinic products. However, the amount of adsorbate changes as a function of temperature. This is shown in Fig. 7. A 4:1 ratio of the carbon 274 eV Auger peak to the platinum 238 eV Auger peak corresponds to a complete monolayer of carbon by calibration with acetylene. The carbon coverage ranges from 0.1 monolayer at 300 K to almost 1.0 monolayer at 723 K. The line has a slope of 2 ± 0.2 kcal/mole. During and after the reaction this carbon deposit was always present on the surface not only at our low pressure reaction conditions, but also after reactions that were carried out in another apparatus at higher pressures (*9*) (approx 200 Torr total pressure).

The temperature dependence of the dehydrogenation and hydrogenolysis rates for the various crystal faces at a fixed hydrogen to hydrocarbon ratio of 20:1 is shown in Fig. 8. The dehydrogenation rate to benzene decreases with increasing temperature, reaches a minimum of 573 K, then increases slightly at 723 K. The rate of formation of olefinic products have a similar temperature dependence as that of the rate of formation of benzene. The hydrogenolysis rate to saturated products increases with increasing temperature and an Arrhenius plot gives an activation energy of 3 ± 0.3 kcal/mol that is the same for all of the crystal faces within our experimental accuracy.

We have found that the dehydrogenation reaction of cyclohexane to form benzene was sensitive to the ordering of the carbonaceous overlayer as shown in Fig. 9. Initially, the overlayer was ordered on all of the stepped surfaces that were studied and dehydrogenation yielded more benzene

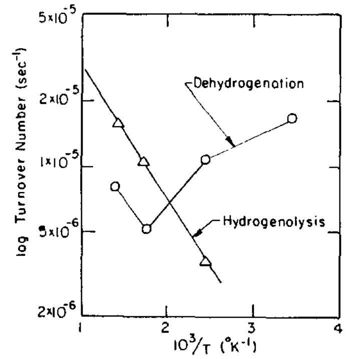

FIG. 8. Temperature dependence of dehydrogenation of cyclohexane to benzene (○) and hydrogenolysis (△). The overall activation energy for hydrogenolysis is 3 ± 0.5 kcal/mole. Standard reaction conditions, data for Pt(S)-[6(111)×(100)].

than cyclohexene. The low-energy electron diffraction pattern from the carbon deposit formed on stepped surfaces in 20:1 hydrogen to hydrocarbon reaction mixture at 423 K and above has a hexagonal unit cell approximately 5.1 Å on a side. This is about 5% larger than the next nearest neighbor distance of Pt and considerably smaller than the Van der Waal's radius of either benzene (7.2 Å) or cyclohexane (7.6 Å) indicating that the adsorbed layer is at least partially dehydrogenated and the diffraction pattern is certainly not due to the intact reactant or product molecules. Complete dehydrogenation that occurs on heating the adsorbed layer to above 1000 K yields graphitic deposits characterized by ring-like diffraction features of 2.46 Å unit cell size (*10*). The platinum diffraction features after a reaction are readily visible and identical to those from the clean surface (except Pt(S)-[7(100) × (111)] where the surface reconstruction disappears) (*4*). The diffuseness of the extra diffraction features correlates with the terrace width, sharper spots on wider terraces (*11*). This and the different diffraction pattern on the Pt(111) surface indicate the formation of the carbon overlayer is intimately associated with the steps. After several hours of reaction time, the carbonaceous overlayer slowly disorders. Simultaneously, the rate of production of cyclohexene increases while the rate of benzene formation decreases until the product becomes predominantly cyclohexene. As shown in Fig. 9 for the Pt(S)-[6(111) × (100)] surface at 423 K, the initial 2:1 benzene to cyclohexene product ratio typical for dehydrogenation on ordered carbonaceous overlayers becomes 1:3 on a disordered overlayer. Thus, for all practical purposes, the dehydrogenation on disordered overlayers produces cyclohexene as further dehydrogenation to benzene is poisoned.

A small amount of oxygen on a stepped surface is an effective poison for dehydrogenation. If the catalyst sample was not vacuum reduced at 1375 K after oxygen cleaning, approximately 0.1 of a monolayer of oxygen (by Auger electron spectroscopy) would be left on the catalyst. This was enough to completely stop the production of benzene and decrease the cyclohexene production by 50% at 423 K on the Pt(S)-[6(111) × (100)]. The low-energy electron diffraction features were identical to Fig. 3a, but the background intensity was higher. The 0.1 monolayer coverage would be less than one oxygen atom per step atom if all the oxygen was adsorbed at the steps. (But, since the cyclohexene production is decreased as well as the benzene production, there may be some oxygen on the terraces as well as at the steps.) The oxygen was still present on the surface after 1 hr of reaction at 423 K and standard pressure conditions.

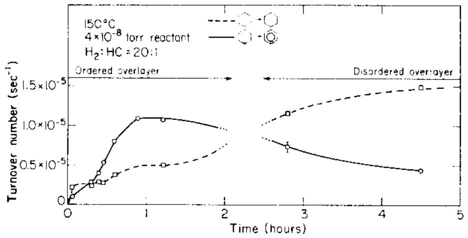

FIG. 9. Inhibition of benzene (○) from cyclohexane and increase in cyclohexene formation (□) with time on Pt(S)-[6(111) × (100)] surface. All catalysts with (111) orientation terraces behave similarly.

B. The Dehydrogenation and Hydrogenolysis of Cyclohexene

The turnover number for the dehydrogenation of cyclohexene to benzene is about two orders of magnitude greater than for the dehydrogenation of cyclohexane. In Fig. 10a we plot the dehydrogenation rate as a function of step density. The turnover number increases rapidly with step density indicating that unlike the slower dehydrogenation reaction of cyclohexane, this reaction is structure-sensitive. In Fig. 10b

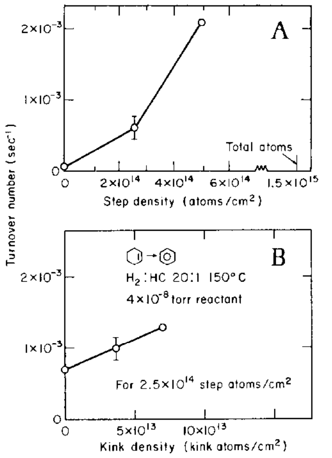

FIG. 10. Cyclohexene dehydrogenation to benzene as a function of: (A) step density and (B) kink density. Standard reaction conditions.

the turnover number is plotted as a function of kink density. Although there is a small increase in the dehydrogenation rate, it may be considered insignificant compared to the marked change of rate with step density. The rates in Fig. 10 are the maxima of the deactivation curves as depicted in Fig. 11.

Unlike the dehydrogenation of cyclohexane, the cyclohexene dehydrogenation reaction poisons rapidly on many catalyst surfaces. Using a hydrogen to cyclohexene mixture of 20:1, the rate of dehydrogenation reaches a maximum, then it decreases rapidly as poisoning occurs, the catalysts losing approximately one-half of their activity in 10–12 min. Figure 11 shows a representative plot of the turnover number as a function of time. On many catalyst surfaces, particularly on those with (111) orientation terraces, a disordered carbonaceous overlayer forms which poisons further dehydrogenation of cyclohexene. The poisoning is greatly decreased, however, if the carbonaceous overlayer is ordered.

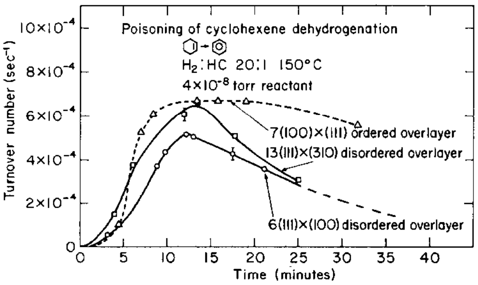

FIG. 11. Inhibition of benzene formation from cyclohexene on disordered carbonaceous overlayers (——), Pt(S)-[6(111) × (100)] and Pt(S)-[13(111) × (310)]; and lack of inhibition on ordered carbonaceous overlayer (- - -), Pt(S)-[7(100) × (111)].

The overlayer is disordered on (111) orientation terraced stepped surfaces while the overlayer orders on surfaces with (100) orientation terraces upon cyclohexene–hydrogen adsorption at 423 K. With an ordered overlayer, the rate of dehydrogenation remains high longer and there is only slow deactivation of these catalysts. On both types of catalyst surfaces the coverage is approximately 1.0 monolayer of carbon after the induction period.

DISCUSSION

A. *Active Sites for C–H, H–H, and C–C Bond Breaking*

Dehydrogenation of cyclohexane and cyclohexene to benzene occurs readily at low pressures (less than 10^{-6} Torr) on stepped platinum catalyst surfaces. This is in contrast with the very slow or negligible dehydrogenation rate of these molecules on the Pt(111) catalyst surface (*1*). Thus, C–H bond breaking takes place at atomic steps, the same steps that are effective in breaking H–H bonds as revealed by studies in this laboratory of the hydrogen–deuterium exchange reaction at low pressures, using molecular beam scattering techniques (*2*). Atomic steps on platinum surfaces appear to be the active sites for C–H and H–H bond scissions.

We have been able to identify another active site by studying the ratio of the dehydrogenation rate to hydrogenolysis rate of cyclohexane to benzene and *n*-hexane, respectively. While the benzene:*n*-

hexane ratio is 3:1 on a stepped surface (with roughly 17% of the surface atoms in step positions), the ratio decreases rapidly with increasing kink density (Fig. 5b). Using a set of catalyst surfaces that were cut to maintain the same terrace width (step density equal to $2.5 \times 10^{14}/\mathrm{cm}^2$), but with variable kink density in the steps, we have found that the hydrogenolysis rate increases linearly with kink density while the dehydrogenation rate remains unaffected. On a Pt(S)-[7(111) × (310)] catalyst surface approximately 30% of the atoms in the step are in kink positions (in addition to the thermally generated kinks). For this surface the benzene to *n*-hexane ratio has reached unity. Thus, the microstructure of kinks in the steps is effective in breaking C–C bonds in addition to C–H and H–H bonds. The selectivity of these bond breaking processes at different atomic surface sites on platinum is certainly significant in that the atomic surface structure of platinum may be properly tailored to provide selectivity in chemical reactions where C–H and C–C bond breaking processes are to be separated.

B. The Carbonaceous Overlayer

During dehydrogenation of cyclohexane and cyclohexene, the platinum crystal surfaces are always covered with a carbonaceous deposit of 0.1–1.0 monolayer judged by the carbon to platinum Auger peak intensity ratio. The coverage appears to increase with increasing reaction temperature, but is rather independent of pressure as indicated by recent high pressure studies on the Pt(S)-[6(111) × (100)] catalyst surfaces in this laboratory (*9*). The overlayer coverage also depends on the particular surface reaction, higher molecular weight reactants and products (cyclohexene, benzene, *n*-heptane, toluene) yield greater coverage than low molecular weight reactants and products (cyclopropane, propane, etc.). Low molecular weight hydrocarbons (cyclopropane, ethane) which do not form carbonaceous overlayers do not readily react on platinum surfaces at low pressures. The build-up of adsorbates during the induction period for cyclohexane and cyclohexene dehydrogenation to benzene indicates the need for the formation of a carbonaceous overlayer to obtain the products. This is not a build-up of the product benzene since it will desorb at a two orders of magnitude higher rate as evidenced by the rate of cyclohexene dehydrogenation.

During the dehydrogenation of cyclohexane the carbonaceous overlayer is ordered initially. After a few hours of reaction at 423 K, however, the overlayer becomes successively more disordered as judged by its low-energy electron diffraction pattern. The amount of carbon in the overlayer, however, remains constant at approximately 0.3 monolayers as determined by Auger electron spectroscopy. Simultaneously the product distribution in the dehydrogenation reaction changes as well. While benzene is the dominant product in the presence of the ordered overlayer, cyclohexene becomes the major product of the dehydrogenation reaction in the presence of the disordered overlayer. This is shown in Fig. 9. Thus, the disordering of the carbonaceous overlayer poisons the formation of benzene, i.e., the dehydrogenation of cyclohexene, and under the reaction conditions the cyclohexene intermediate becomes the final product. It should be noted that the turnover number for the cyclohexene–benzene reaction is two orders of magnitude higher (approx 10^{-3}/sec) than for the cyclohexane–benzene reaction (approx 10^{-5}/sec). Thus, the presence of the disordered overlayers poisons the fast second step, but not the first slow step in the dehydrogenation of cyclohexane to benzene.

The marked effect of the ordering characteristics of the carbonaceous deposit on the reaction rate is also clearly displayed during our studies of the dehydrogenation of cyclohexene. As shown in Fig. 11, there is rapid poisoning of the dehydrogenation rate within minutes as the disordered carbonaceous overlayer forms. However, when the overlayer is ordered [on (100) orientation terraced surfaces], the catalytic activity decreases much more slowly. Again, the poisoning of benzene production is prevented by the formation of an ordered overlayer. Since the platinum catalyst surface is covered with a carbonaceous layer at low as well as at high pressures, we must consider this layer an important part of the surface reaction.

Carbonaceous overlayers can have an important effect in both the catalytic activity and selectivity of a metal surface. Weinberg *et al.* (*12*) postulated that the carbonaceous overlayer is the catalytic site for the hydrogenation of ethylene on the Pt(111) surface and similarly, by Gardner and Hansen (*13*) for tungsten stepped surfaces. Yasumori *et al.* (*14*) found preadsorbing acetylene prevents poisoning or restores the activity of a palladium film for the hydrogenation of ethylene. In all three cases, the structure of the carbonaceous overlayer has a marked effect on the catalytic activity in a manner which is not simple site blockage poisoning. Holbrook and Wise (*15*) found a specific pretreatment of their Pd catalyst which involved oxygen activation and hydrocarbon preadsorption could markedly affect the selectivity of an isomerization reaction. The rate of dehydrocyclization of *n*-heptane, as well as the selectivity to isomerization and hydrogenolysis, was observed in this laboratory (*16*) to be dependent on the ordering of the carbonaceous overlayer. These observations, in addition to the data presented in this paper indicate that the formation of the carbonaceous overlayer on the catalyst surface can affect the selectivity as well as activity of a catalytic reaction. The presence of these effects at both atmospheric and low pressure and on a variety of metals indicates the importance of the carbonaceous overlayers and the need for their further characterization. This leads to the conclusion that not all carbon on a catalyst surface is deleterious and only amorphous forms cause site blockage poisoning.

C. The Mechanism of the Dehydrogenation of Cyclohexane and Cyclohexene; Expanded Classification of Reactions According to Their Structure Sensitivity

In dispersed metal catalysts, the metal is dispersed into small particles, the order of 5–500 Å in diameter, which are generally located in the micropores (20–1000 Å) of a high surface area support. This provides a large metal surface area per gram for high, easily measurable reaction rates, but hides much of the structural surface chemistry of the catalytic reaction. The surface structure of the small particles is unknown; only their mean diameter can be measured and the pore structure could hide reactive intermediates from characterization. Some of the same difficulties also hold for thin films. However, we can accurately characterize and vary the surface structure of our single crystal catalysts and in our reactor reactive intermediates can be readily measured; both are prerequisites for the mechanistic study of the catalysis on the atomic scale.

We have been able to identify two types of structural features of platinum surfaces that influence the catalytic surface reactions: (a) atomic steps and kinks, i.e., sites of low metal coordination number and (b) carbonaceous overlayers, ordered or disordered. The surface reaction may be sensitive to both or just one of these structural features or it may be totally insensitive to the surface structure. The dehydrogenation of cyclohexane to cyclohexene appears to be structure-insensitive reaction. It takes place even on the Pt(111) crystal face that has a very low density of steps and proceeds even in the presence of a disordered overlayer. The dehydrogenation of cyclohexene to benzene is very structure-sensitive. It requires the presence of atomic steps (does not occur on the Pt(111) crystal face) and the presence of an ordered overlayer (it is poisoned by disorder). Others have found the dehydrogenation of cyclohexane to benzene to be a structure-insensitive (*17–21*) reaction on dispersed metal catalysts. On our catalyst, surfaces which contain steps, this is also true, but on the Pt(111) catalyst surface, benzene formation is much slower. Dispersed particles of any size will always contain many step-like atoms of low coordination, and therefore, the reaction will display structure-insensitivity. Based on our findings, we may write a mechanism for these reactions by identifying the sequence of reaction steps:

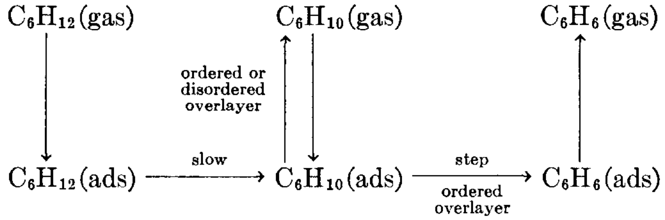

The slow step in the dehydrogenation of cyclohexane to benzene is the production of the cyclohexene intermediate at these low pressures on stepped surfaces. Cyclohexene dehydrogenates very rapidly at a *step* to form benzene; approximately 1 in every 3 collisions of a cyclohexene molecule with an unpoisoned step results in the formation of a benzene molecule. However, on the Pt(111) surface, which is practically free of steps, the rate of dehydrogenation of cyclohexene had become slow enough to be rate-limiting (*1*). Sinfelt *et al.* (*22*) concluded the dehydrogenation of methylcyclohexane to toluene, a very similar reaction to cyclohexane dehydrogenation to benzene, was rate limited by the desorption of toluene. The rate controlling step is probably different at the conditions (several atmospheres pressure) of their experiments. Maatman *et al.* (*19*) postulated the slow step, in agreement with our results, as the formation of an intermediate species. Haensel *et al.* (*23*) have observed the intermediate cyclohexene species at very high (approx 30,000 LHSV) space velocities. This indicates the intermediate is also found at atmospheric pressure reaction conditions. Near surface equilibrium (low space velocities) the cyclohexene intermediate is not observable since it is very reactive at the step and edge atoms which must exist on the dispersed metal particles.

In addition to dehydrogenation reactions, hydrogenolysis is also taking place on the platinum surfaces. By monitoring the benzene to *n*-hexane ratio on the various catalysts as a function of surface structure, we have identified steps as primarily responsible for C–H and H–H bond breaking and kinks for C–C bond breaking in addition to C–H and H–H bond scissions. Thus, hydrogenolysis is initiated at kinks in the atomic steps. Since we need specific surface sites for hydrogenolysis to occur this is also a structure-sensitive reaction. However, hydrogenolysis is insensitive to the state of ordering of the carbonaceous overlayer. It proceeds whether the carbonaceous overlayer is ordered or disordered.

It appears that the classification of structure-sensitive reactions (*24*) should be expanded to separate those reactions

TABLE 2

Classification of Reactions by Step Density and Carbonaceous Overlayer Dependence

Step structure-sensitive		Step structure-insensitive	
Overlayer structure sensitive	Overlayer structure insensitive	Overlayer structure sensitive	Overlayer structure insensitive
Cyclohexene → benzene *n*-Heptane → toluene	Cyclohexane → *n*-hexane		Cyclohexane → cyclohexene Cyclopropane → propane

that exhibit step (or kink) sensitivity into one group and those that are also sensitive to the structure of the overlayer, into another group. This expanded classification is shown in Table 2. In addition to the dehydrogenation and hydrogenolysis reactions described in this paper we have included two other reactions that were studied recently (*16*, *25*). It would be of great value to include in this classification several other hydrocarbon reactions (isomerization, hydrogenation, exchange). More reactions are presently being studied to expand these results on characterized surfaces. Monogue and Katzer (*26*) have proposed a subdivision of structure-sensitive (demanding) reactions along very similar lines. "Primary structure-sensitivity" is the effect of changing particle size or step and kink density. Their "secondary structure-sensitivity" includes effects of self-poisoning and oxygen impurity on reaction rate. The self-poisoning phenomena is, for hydrocarbon reactions on platinum, at least at low pressure, the sensitivity of a reaction to the order in the carbonaceous overlayer. However, caution must be exercised in studies of structure-sensitivity as the reaction mechanism or the surface structure may change markedly with pressure, temperature, and reactant ratio. Most of the surface structure-sensitivity of various catalytic reactions was derived from the particle size dependence of the reaction rate on polydispersed metal catalyst systems. Although there is excellent agreement between the classifications of the various reactions based on studies using supported metal catalysts with variable particle size and our studies using various single crystal surfaces, this may not be the case for all reactions. Perhaps the step density or the kink density is proportional to particle size while the ordering characteristics of the carbonaceous overlayer may or may not be affected by changes of particle size. In addition, studies similar to those reported on platinum must be carried out using crystal surfaces of other transition metals to ascertain that these arguments are more broadly applicable to describe the catalytic chemistry of transition elements. There is evidence that the heat of adsorption of hydrogen on palladium crystal surfaces varies markedly with step density (*27*) while gold crystal surfaces exhibit chemisorption behavior that is independent of step density (*28*).

D. A Descriptive Model of Hydrocarbon Catalysis on Platinum Surfaces

Studies to correlate the reactivity and the surface structure and composition of platinum surfaces indicate that the active platinum crystal surface must be heterogeneous. The heterogeneity involves the presence of various atomic sites that are distinguishable by their number of nearest neighbors (atoms in terraces, in steps and in kinks), and also variation in surface chemical composition. A model that depicts the active platinum surface is shown schematically in Fig. 12. Part of the

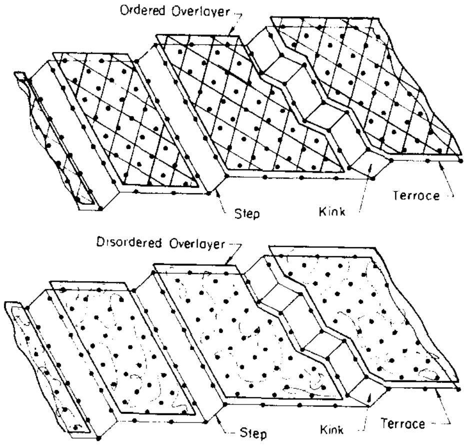

FIG. 12. Schematic representation of a platinum catalyst with a monolayer of carbonaceous overlayer showing the exposed platinum clusters.

surface is covered with a partially dehydrogenated carbonaceous overlayer, ordered or disordered, from which "islands" of platinum clusters protrude. These are the platinum atoms in steps and at kinks that are active in various C–C, C–H, and H–H bond breaking activity. Perhaps because of the ease of dissociation and higher binding energy of hydrogen at the steps, these sites and their vicinity remain clean and represent areas of high turnover number. The species that form as a result of bond scission at these clusters may rearrange and then diffuse away onto the terrace that is covered with the overlayer, where desorption takes place. Alternately, rearrangement takes place on the ordered carbonaceous overlayer prior to desorption. The heat of desorption should be lower on the portion of the surface that is covered with the overlayer than at an exposed step.

The discovery that kink sites in steps are effective in breaking C–C bonds in addition to C–H and H–H bonds, thereby initiating hydrogenolysis reactions may also explain the effect of trace impurities or second component metals that introduce selectivity. Since these kink sites have fewer nearest neighbors than step or terrace sites, they are likely to bind impurities or other metal atoms with stronger chemical bonds. Thus, these sites are readily blocked by impurities. As a result selective "poisoning" of hydrogenolysis may be obtained by minute concentrations of well-chosen impurities or another metal component.

ACKNOWLEDGMENTS

This work was supported by the U. S. Energy Research and Development Administration, the Petroleum Research Foundation (6059-AC5), and the Mobil Research Corporation. We are grateful to Dr. Ch. Steinbrüchel for numerous suggestions.

REFERENCES

1. Gland, J. L., Baron, K., and Somorjai, G. A., *J. Catal.* **36**, 305 (1975).
2. Bernasek, S. L., and Somorjai, G. A., *J. Chem. Phys.* **62**, 3149 (1975).
3. Lang, B., Joyner, R. W., and Somorjai, G. A., *Surface Sci.* **30**, 440 (1972).
4. Morgan, A. E., and Somorjai, G. A., *Surface Sci.* **12**, 405 (1968).
5. Blakely, D. W., and Somorjai, G. A., to be published.
6. Henzler, M., *Surface Sci.* **19**, 159 (1970); **22**, 12 (1970).
7. Williams, F., and Boudart, M., *J. Vac. Sci. Technol.* **9**, 362 (1972).
8. Levenspiel, O., "Chemical Reaction Engineering." Wiley, New York, (1962).
9. Herz, R., private communication.
10. May, J. W., *Surface Sci.* **17**, 267 (1969).
11. Park, R. L., and Houston, J. E., *Surface Sci.* **18**, 213 (1969); Park, R. L., Houston, J. E., and Schreiner, D. G., *Rev. Sci. Instrum.* **42**, 60 (1971).
12. Weinberg, W. H., Deans, H. A., and Merrill, R. P., *Surface Sci.* **41**, 312 (1974).
13. Gardner, N. C., and Hansen, R. S., *J. Phys. Chem.* **74**, 3298 (1970).
14. Yasumori, I., Shinohara, H., and Inoue, Y., *in* "Catalysis" (J. Hightower, Ed., North-Holland, Amsterdam, 1972).
15. Holbrook, C. M., and Wise, H., to be published.
16. Lang, B., Joyner, R. W., and Somorjai, G. A., *J. Catal.* **27**, 405 (1972); L. B. L. Report 2796, unpublished data; Blakely, D. W., PhD thesis, Univ. of California-Berkeley, 1975.
17. Poltorak, O. M., and Boronin, V. S., *Zh. Fiz. Khim.* **40**, 2671 (1966).
18. Mitrofanova, A. N., Boronin, V. S., and Poltorak, O. M., *Zh. Fiz. Khim.* **46**, 32 (1972).

19. Maatman, R. W., Mahaffy, P., Hoekstra, P., and Addink, C., *J. Catal.* **23**, 105 (1971).
20. Cusamano, J. A., Dembinski, G. W., and Sinfelt, J. H., *J. Catal.* **5**, 471 (1966).
21. Kraft, M., and Spindler, H., *Proc. Int. Congr. Catal. 4th, 1968* **2**, 286 (1971).
22. Sinfelt, J. H., Hurwitz, H., and Shulman R. A. *J. Phys. Chem.* **64**, 1559 (1960).
23. Haensel, V., Donaldson, G. R., and Riedl, F. J., *Proc. Int. Congr. Catal., 3rd, 1964* **1**, 294 (1965).
24. Boudart, M., Aldag, A., Benson, J. E., Dougarty, N. A., and Harkins, C. Girvin, *J. Catal.* **6**, 92 (1966).
25. Kahn, D., Peterson, E. E., and Somorjai, G. A., *J. Catal.* **34**, 294 (1974).
26. Manogue, W. H., and Katzer, J. R., *J. Catal.* **32**, 166 (1974).
27. Conrad, H., Ertl, G., and Latta, E. E., *Surface Sci.* **40**, 435 (1974).
28. Chesters, M., and Somorjai, G. A., *Surf. Sci.* **52**, 21 (1975).